Spatial Resolution of Solar Total Irradiance Variability: The *YOHKOH* White–Light Observations

By HUGH S. HUDSON

Institute for Astronomy, Honolulu, HI 96822, USA

The observations from the ACRIM instrument on board the *Solar Maximum Mission*, and other recent experiments, have allowed us to study the time variations of solar irradiance. These observations identified several mechanisms, ranging from sunspots to global oscillations produced by waves trapped in the solar interior (the p-modes) that cause variations in the total irradiance. In all cases the variations have small amplitudes in integrated light from the visible photosphere. The SXT instrument on board *Yohkoh* has provided a new data set that can resolve some of these variations spatially. Most of these data are in the form of whole-Sun images: rate about 5 per day; effective pixel size of 4.92 arc sec; passband 28Å centered at 4310Å; data interval beginning in September, 1991 and ending in October, 1992. These observations have several advantages over ground-based observations for the characterization of solar global variability, namely the lack of atmospheric effects and the long-term stability of the instrumentation. We present an assessment of these data in the context of the existing total irradiance data, and also discuss their application to determination of the figure of the Sun, particularly measurements of the variations of the solar radius.

1. Introduction

The ACRIM instrument on board *Solar Maximum Mission* greatly stimulated interest in the solar irradiance from two points of view: both as the defining forcing agent for climate change on Earth, and as a means of learning about the solar interior via inferences regarding the mechanisms of solar luminosity variability (*e.g.* Newkirk 1983). ACRIM and other total irradiance instruments detected variability on a wide range of time scales, up to the length of the present time series (for reviews see Hudson 1988; Fröhlich *et al.* 1991). Observations from the entire disk of the Sun confuse all of these mechanisms of solar variability. Thus time-resolved imaging observations, with high photometric accuracy, clearly would help in understanding the physics of at least some of the processes involved. Observations from space would be preferred for this purpose, although ground-based observations also hold a great deal of promise — for spatially resolved data, ground-based image photometry can be normalized to the whole Sun, and thus avoid many photometric problems.

The history of solar imaging at optical wavelengths from space is quite limited. About the only observations have been the balloon-borne telescopes (*e.g.*, Danielson 1961) and the time series of optical images from the SOUP experiment on *Spacelab-2* (*e.g.*, Title *et al.* 1989). This paper centers on the observations from the aspect camera of the SXT instrument on board *Yohkoh*, which has provided the first lengthy time series of solar white-light images from space. These data can be used in studies of the development of solar activity, the figure of the Sun, the limb distribution of surface brightness, g-modes, flares, solar rotation, etc. For a review of the *Yohkoh* X-ray observations, see Shibata (1994).

This paper tries to describe the properties of the data and the observing system, and in doing so it lists all the problems that we know about. The reader should not construe

https://doi.org/10.1017/S0252921100024696 Published online by Cambridge University Press

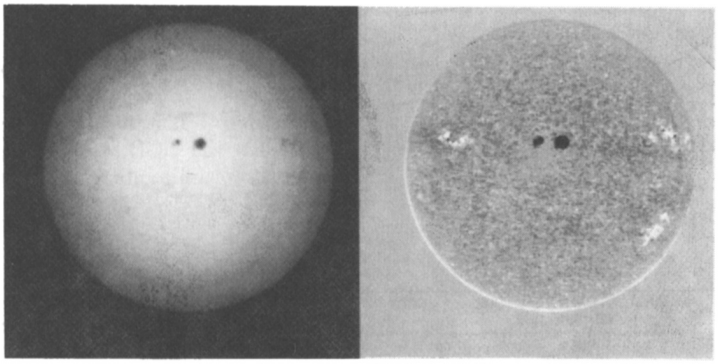

FIGURE 1. Image of the Sun obtained from the SXT instrument on board the *Yohkoh* spacecraft. Left, raw data; right, residuals as described in Section 4. This image (N top, E left, pixel size 4.92 arc s square, exposure time 0.339 ± 0.004 s) is from 03:27:36 UT, 18 August 1992. The large spot group is NOAA active region 7260, with a tabulated area of 940 millionths. The observations were made in the *Yohkoh* "narrow-band" filter, 28Å bandwidth centered at 4310Å.

this negatively. These data are unique and will be used in many important applications in the future. The CCD detector and optical system of the *Yohkoh* instrument clearly cannot produce the remarkable photometric stability displayed by ACRIM-type sensors, but the spatially resolved variations have much larger relative amplitudes.

2. The *Yohkoh* white-light data base

The SXT instrument on *Yohkoh* (see Tsuneta *et al.* 1991, for a general description) provided white-light observations of the solar disk as a byproduct of its primary function of soft X-ray imaging. The main purpose of these white-light images is to provide coalignment information for the X-ray observations via sunspot locations relative to the limb. The time series began in September 1991, and ended in October, 1992. The essential part of the database consists of about thirteen months of routine observations. The total number of images such as that of Figure 1 exceeeded 2,000 over this time interval, corresponding to a rate of approximately five per day.

The white-light images come from a 1024 × 1024 virtual-phase CCD illuminated by a 5-cm lens. The telescope has a fixed focus maintained by a graphite-epoxy metering structure, with the focus established by observations in Palo Alto, California, before launch. Most of the data reported here come from 2 × 2 pixel summations, resulting in an effective pixel size of 4.92″, and were synthesized from two separate exposures in order to extend the 8-bit telemetry to 12 bits. Limited amounts of full-resolution data are available, almost always during "flare mode." This resulted in stretches of data with approximately one image each 10-12 s, but over a restricted field of view of 64 × 64 pixels (about 2.62′ square). Note that the pixelization does not critically sample the spatial structure of the image ($1.22\ \lambda/d = 2.17''$), so that relatively large pixel-to-pixel variations may occur. The optical layout seems quite simple, consisting of the lens, blocking filters, and bandpass filters isolating one of two spectral bands, but the Appendix gives the flavor of some of the problems encountered in making it work properly. The data reported here come mainly from a filter with a nominal bandpass of 28Å centered at 4310Å. This is in

https://doi.org/10.1017/S0252921100024696 Published online by Cambridge University Press

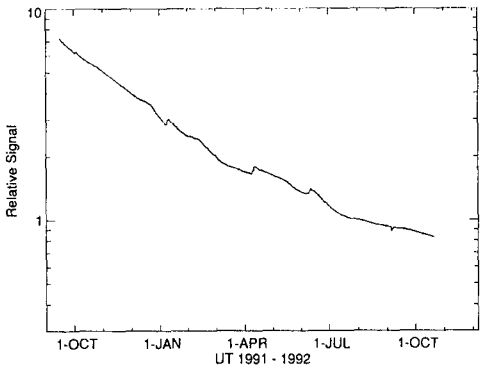

FIGURE 2. Relative signal level for *Yohkoh* white-light images, showing the steady decrease of signal level during the duration of the observations. The necessary exposure time grew from about 60 msec to about 948 msec during this period. The sudden increases occurred when the CCD was warmed up to drive off contaminants from its surface.

the Fraunhofer G band and was chosen for the aspect-sensing function of SXT in order to show the chromospheric network and faculae.

The aspect telescope performed well until the loss of an X-ray aperture filter in October 1992, which "blinded" the optical system with visible light reflected off the X-ray optics. In orbit the CCD slowly became contaminated, possibly as a result of the dehydration of the telescope's metering structure. This effect probably presents the most serious problem for precise analyses of these data, because the contamination has fine spatial structure of relatively large amplitude and also varies with time. Periodic heating of the CCD, at intervals of one to two months, drove some of the contamination off.

There was also a continual loss of sensitivity over the total span of the data, as shown in Figure 2. This quasi-exponential decay, which could be localized to the pre-filter/lens assembly, resulted in gradually increasing exposure times as the mission went on. Finally, we also observed a gradual degradation of the "flat-field" map, which was routinely observed using sunlight through a diffusing glass filter. None of these problems seriously affected the use of the data for aspect sensing, and it remains to be seen how much they will impact the scientific use of the data.

The images are nominally oriented to solar north by *Yohkoh*, but there are limited intervals during which this system was not maintained well and the N orientation wandered a small amount. There is also a one-year periodic error with an amplitude of approximately 0.45°, due to the on-board ephemeris for the Canopus reference sensor (T. Kosugi, personal communication).

Figure 3 compares "flat-field" maps derived from routine diffuse-light images, illustrating the changes in the spatial flatness of the response during the period of observation. This resulted from an unanticipated degradation of the CCD surface layers by the same soft X-radiation that SXT was designed for (fortunately, the degradation does not appear to have affected the X-ray response). The flat-field maps therefore reflect a kind of time integral of the detected X-ray flux, including some artifacts of individual flares that were not intercepted by the *Yohkoh* flare trigger and for which the X-ray exposure times were therefore not properly adjusted downwards by the automatic exposure-control logic. The detailed appearance of the flat-field maps can also be derived from the white-light data directly, by using the stability of the solar brightness distribution in the mean (A. McAllister, private communication). For the central region of the Sun, this may be the preferred technique for future studies of these data, since the flat-field irregularities shown in Figure 3 eventually became deeper than 20% near the limb positions, and because the diffuser flats do not have the same passband as the two analysis filters.

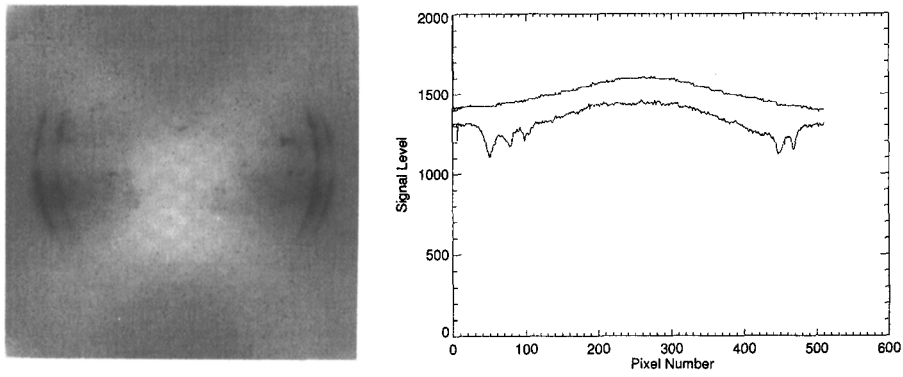

FIGURE 3. Flat-field image (N top, E left) obtained from near the end of the *Yohkoh* white-light data interval, 21 October 1992. The large-scale structure comes from the optics of the opal glass diffuser used to provide the illumination, and has an amplitude of a few percent; the small-scale structure comes from radiation damage to the CCD induced by the solar soft X-rays. The pattern represents a time integral over the whole mission, so that one can see the effects of pointing changes of the spacecraft, and even of individual bright flares. This damage has no appreciable effect on the X-ray sensitivity of the detector. The line plot on the right compares the flat-field structures from this image with one taken a year earlier, 31 October 1991 (plot shows the middle row of the 512 × 512 pixel images).

3. The solar radius

One of the initial engineering analyses involved measuring the apparent location of the solar limb. This was essential for SXT image registration. The results from this analysis are described in this section. The program (FIND_LIMB) used for this purpose is unsophisticated, consisting of an image differentiation based on the "Sobel" filter: $G(i,j) = \sqrt{(X^2 + Y^2)}$, in an approximation (from the IDL library) that defines X and Y as functions of the values in the eight pixels surrounding the (i,j)-th pixel. The differentiated image is subjected to various tests designed to screen out artifacts due to charged particles and to sunspots. The coordinates of the individual pixels of the differentiated image that pass these tests are then analyzed harmonically as a function of azimuth angle around the limb. FIND_LIMB returns the coordinates of the center of the image, the radius, a value for the scatter of the radius pixels around the best-fit limb trace, plus higher-order harmonic terms. The limb location defined in this way does not include effects due to the limb-darkening function at the extreme limb, and in this manner retains some direct sensitivity to low-level distortions of the limb-darkening function resulting from faculae. The use of the 4310Å filter for the bulk of these data probably enhances this effect, but it is also present in the SXT "broad-band" filter (184Å centered at 4616Å).

The current precision of the radius determination from a single image is about 0.1 arc s (rms) on short time scales, as determined by the scatter of the individual measurements. This compares favorably with the best ground-based observations (the H.A.O. observations of T. Brown) quoted by Ribes *et al.* (1991) to be ~0.14 arc s per day. The relatively short span of the *Yohkoh* data makes it difficult to compare these observations with longer runs of ground-based observations of the solar radius, at least in terms of the slow variations that have been reported by the CERGA group and others (Ribes *et al.*

https://doi.org/10.1017/S0252921100024696 Published online by Cambridge University Press

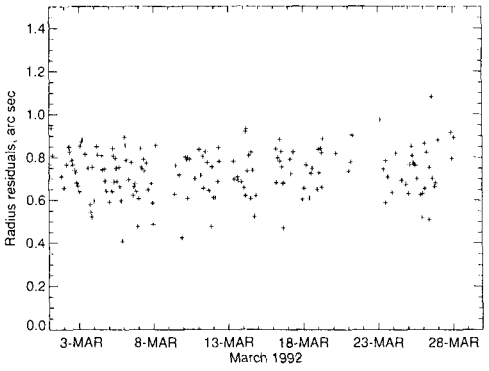

FIGURE 5. Apparent variation of solar radius determined from the SXT white-light images for the entire span of the data (upper). The lower panel shows the variation of sunspot number over the same time interval. The apparent solar radius decreased by about 0.7 arc s in coincidence with the decrease of solar activity in early 1992.

FIGURE 4. Apparent variation of solar radius determined from the SXT white-light images for one month in 1992.

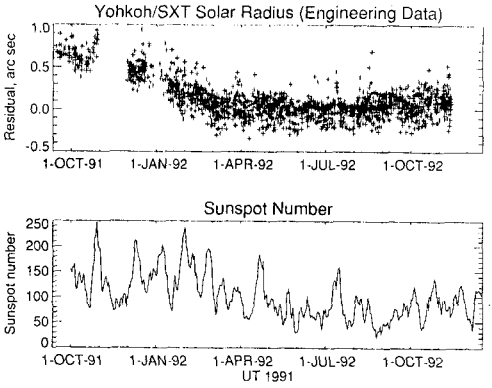

1991). Overlapping data exist but have not yet been jointly analyzed. The short-term scatter of these SXT radius determinations is considerably greater than theoretical limits imposed by pixelization or counting statistics (Buffington *et al.* 1991), but Figure 4 suggests that this scatter is approximately random.

On longer time scales the SXT radius determinations, made as described above, show a systematic variation (Figure 5). There is a clear variation of apparent solar radius with time, roughly correlated with the general level of solar activity as shown by the sunspot number. One possible cause of this observed variation, if solar in origin, could be confusion of facular brightness variations with true figure variations. Equally likely would be systematic errors of observation that coincidentally resemble the sunspot number variation. These data show a larger apparent radius variation than any present in the H.A.O. monthly means for 1981–1988. This paper cannot report a definitive conclusion here, and it remains possible that all or a part of the observed apparent radius change results from a true spatial effect. The stability of the measurements suggests that a more careful analysis of these data will provide better limits on true radius variations.

4. The brightness distribution

The main observational goal here consists of tracking the time variations of solar irradiance on a spatially resolved basis, for example to follow an individual active region across the disk and thus to determine the time dependence of the sunspot irradiance deficits and facular excesses (Willson *et al.* 1981). The discussion below describes the properties of the data relative to this goal.

The *Yohkoh* white-light images require dark subtraction and correction for flat-field imperfections. Routine operations of *Yohkoh* provide many dark and diffuser frames with which to make these corrections. Some pixels are "hot", with high dark-current rates;

https://doi.org/10.1017/S0252921100024696 Published online by Cambridge University Press

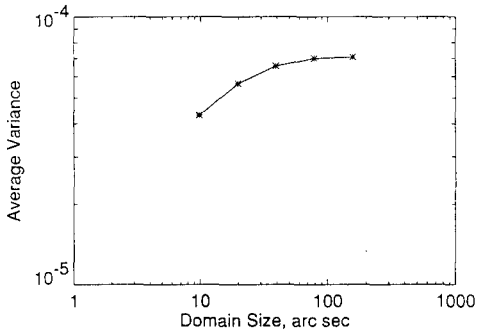

FIGURE 6. Statistics of image structure in a region $5.24' \times 5.24'$ from the image in Figure 1, after flat-fielding and subtraction of a mean image free of sunspots. The plot shows the increase of pixel-to-pixel variance with increasing domain size.

the images are improved cosmetically by dark subtraction, but the noise fluctuations remain. Individual pixels or groups of pixels often show cosmic-ray tracks. Such effects of course cannot be removed except on a case-by-case basis, for example by filtering the image to eliminate pixels that look wrong. For the time of the image in Figure 1, the flat-field map had a total range of 34% and an rms fluctuation of 3.7% of the mean value.

Each of the images in the time *Yohkoh* series should be dark-subtracted, flat-fielded, and reduced to residuals according to the empirical limb-darkening function for this system (see Nishikawa 1994, for an example of such image preparation). Such a comprehensive data reduction is not available yet for the *Yohkoh* data, unfortunately. We have assessed the noise properties of the images in a preliminary manner by carrying out dark subtraction, flat-fielding, and subtraction of a mean image, for the whole-Sun images during the disk passage of AR 7260 (August 1992). The mean image was constructed by omitting the pixels containing sunspots from the summation. In a quiet region near disk center, these procedures resulted in a standard deviation of approximately 1% of the mean brightness for a single $4.92'' \times 4.92''$ pixel, and did not appreciably increase over a test area as large as $5.24' \times 5.24'$ from the image in Figure 1. This level of variation is consistent with the level expected from p-modes and granulation. The statistics of this test region of Figure 1 are shown in Figure 6. The decrease of fractional variance for larger bin sizes indicates that the sources of the fluctuations remain largely unresolved, and that the image preparation has not left much larger-scale structure in the residuals.

For time-series analysis, the temporal fluctuations of the photospheric structures cause a basic limitation to precise photometry. Since the *Yohkoh* images discussed here have such a low cadence, much of this temporal variation will be aliased and not averaged down. Pointing jitter of the *Yohkoh* spacecraft also contributes in principle to the temporal variations by converting spatial patterns into time-series variations.

Thus far, the main application of time-series analysis of the *Yohkoh* white-light data are in the study of "white-light" flares (Hudson *et al.* 1992) and potentially "black light" flares as well (van Driel *et al.* 1994). Anwar *et al.* (1993) also used these flare-mode data to study rapid motions of sunspots associated with a major flare. The data show that all flares above a certain threshold have clearly detectable optical emission excesses as observed in the 4310Å filter. The contrasts are as large as about 50%, depending upon the flare. We have made a preliminary estimation of the ratio of the contrasts in this filter and near Hα for a flare simultaneously observed at Mees Solar Observatory (Canfield *et al.* 1992), and find that the 4310Å filter had a contrast $\sim$2.2 times as great. The flares thus detected have a strong impulsive-phase component appearing to originate at the footpoints of coronal loops, and also may show longer-lasting emission.

The flare studies typically use difference images over a short time span as a means of

https://doi.org/10.1017/S0252921100024696 Published online by Cambridge University Press

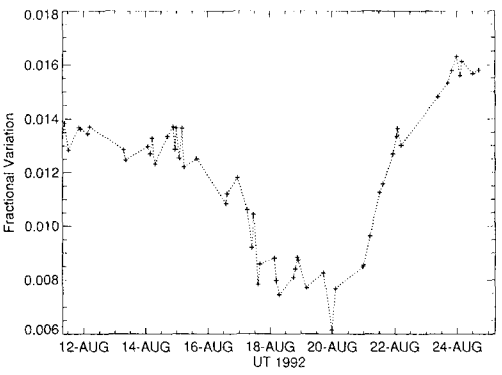

FIGURE 7. Solar brightness variations during the disk passage of NOAA active region 7260 in August, 1992. The plotted data represent the difference between the total signal in a N latitude strip (containing the sunspot group, see Figure 1), and an equivalent S latitude strip. The data are normalized to allow a comparison with the expected total irradiance variation caused by the spot group. The amplitude of the "dip" is larger than what would have been observed by ACRIM I for this sunspot area. This is consistent with the short wavelength (4310Å) of this observation, but detailed comparisons with ACRIM II data need to be made.

levelling the high-contrast features (sunspots) found in active regions. This works well on short time scales, but over the typical span of a "flare mode" observation (about ten minutes) the photospheric background features vary at the level expected from the statistics in Figure 6. Temporal fluctuations on the order of 1% amplitude are present and provide a limiting noise floor for the detection of white-light flare emissions.

We can use the whole-Sun images to study the sunspot "dips" discovered in the ACRIM total irradiance data (Willson *et al.* 1981). Figure 7 shows the effects of the disk passage of the sunspot group of NOAA region 7260. This is the analog of a "dip" in total irradiance as observed by ACRIM. What limits the precision of the photometry reported here? The scatter of individual data points in the time series of Figure 7 exceeds that expected from counting statistics by a large factor. Most of the additional variance must come from unresolved p-modes, granulation, or uncorrected jitter modulation of spatial structures. The latter may be somewhat improved by proper image preparation and rebinning, but the former cannot be escaped without adequate sampling. As Title *et al.* (1989) have shown, the aliasing of the p-modes can be suppressed effectively by spatio-temporal filtering of adequately sampled data. The message for future observations appears to be that the complete spatial resolution of the total irradiance variations will require observations of the whole solar disk at a sufficiently frequent cadence to be able to average down the high-frequency variations induced by waves and convection.

5. Conclusions

The *Yohkoh* data exhibit sufficient precision, stability, and sampling frequency for many of the problems of time-series image photometry needed for the "spatial resolution of the solar variability." To claim this might seem preposterous: the stability of the output of an individual CCD pixel cannot even be known from this data base (but see Buffington *et al.* 1990) very accurately at all, mainly because of the limited number of samples. However one does not even need one-percent photometry per pixel to see the effect of a sunspot as illustrated in Figure 7, much less the far better precision ACRIM demonstrated. I will conclude with a list, not necessarily comprehensive, of observational problems that could be tackled with these data at some future time:

(*a*) Are there novel types of irradiance variability that have not been recognized yet in the ACRIM-type data?

(*b*) Is there evidence for p- or g-modes in the limb figure or photometric data?

https://doi.org/10.1017/S0252921100024696 Published online by Cambridge University Press

(*c*) Are there time-dependent effects in sunspot blocking (*e.g.*, a "thermal shadow" prior to sunspot formation)?
(*d*) Does the solar radius vary with time appreciably?
(*e*) Does the solar limb-darkening function vary with time appreciably?
(*f*) What is the photospheric signature of a coronal hole?
(*g*) What are the limits of detectability of continuum in white-light flares?
(*h*) Are there negative flares?
(*i*) Are flare-related sunspot distortions or motions a common phenomenon?
(*j*) Is there evidence for interplanetary material (*e.g.*, comets) striking the Sun?

These problems touch on several areas in solar physics, with some possibility of elucidating solar interior structure and dynamics. Because scientific studies with a telescope's aspect sensor obviously have secondary importance, it is a tribute to the *Yohkoh* scientific team that the data have such high quality. Even though we are just at the beginning of analysis of these data, I believe that they already demonstrate that spatially resolved irradiance observations can make major contributions. Future instrumentation with more direct optimization for this kind of study would be worthwhile. Based upon the *Yohkoh* experience, the key properties of such observations should include simplicity of optical design, large data throughput, careful control of systematic errors (telescope rotation around the solar direction, desirably), Sun-synchronous or deep-space orbit, careful calibration, and a field of view containing the whole solar disk.

Acknowledgments. I would like to acknowledge the help of many people associated with the white-light capability of SXT and *Yohkoh*: Loren Acton, Marilyn Bruner, Tom Cruz, Sam Freeland, Jim Lemen, Mons Morrison, Bill Rosenberg, Yoshiaki Ogawara, Saku Tsuneta, Bachtiar Anwar, Alan McAllister, Lidia van Driel-Gesztelyi, Dick Canfield and Jean-Pierre Wülser. NASA supported this work under contract NAS 8–37334.

Appendix A. The design of the SXT aspect telescope

The design parameters of the SXT aspect telescope are given in the summary description by Tsuneta *et al.* (1991). Much other material is contained in LPARL SXT Design Note #31 (Grillot & Cruz 1989). The following paragraphs borrows liberally from the latter source and attempts to give all of the relevant unpublished information about the materials and testing of the SXT aspect telescope.

A.1. *Attenuating filters*

The Aspect Telescope consists of an attenuating filter, a bandpass pre-filter, an imaging lens assembly, and four relevant filters in the SXT filter-wheel assembly near the focal plane of the system: an open position, two interference filters for optical wavelength bandpass determination, and an opal glass diffuser used for flat-field calibration of the CCD. See Tsuneta *et al.* (1991) for layout drawings.

The attenuating filter consists of a synthetic fused silica substrate, anti-reflection coated on the sunward surface, with an aluminum attenuating layer on the rear surface. The aluminum thickness is slightly over 500Å, and it has a dielectric overcoating layer for durability. Following this element, there is a bandpass-limiting filter (substrate Hoya CM-500, 6 mm thick). A near-IR coating on the sunward surface of this element was found to attenuate the region from ~4800Å to ~7000Å to 10^{-4} or better. The half-maxima were experimentally determined to be at approximately 3700Å and 4700Å. The transmission of the first elements together was measured to be approximately 1.5×10^{-4}

$\pm$ 5 $\times 10^{-5}$ from approximately 3600Å to 4650Å. The combined out-of-band rejection of the attenuator and bandpass filter together approach or surpass 10^{-8} absolute.

A.2. *Doublet lens*

The visible image is formed by a doublet lens, achromatic across the passband of the entrance filter assembly. The lens has a 50 mm clear aperture and forms a beam at approximately f/31. The doublet has a depth of focus of approximately $\pm$ 0.5 mm, with a fixed focal distance adjusted before flight and an Airy disk diameter about 34 microns.

The sunward element (element #1) of the doublet is a bi-convex lens composed of Schott BK7-G18, a borosilicate crown glass stabilized with cerium. Element #2 of the doublet is a concave-convex lens made from Schott LF5-G15 radiation-damage-resistant flint glass, also cerium-stabilized. The doublet elements are spaced 0.2 mm apart by a stainless steel ring. Both surfaces of both lenses are anti-reflection coated over the passband of the entrance filter. These lenses assist in attenuating incident light at wavelengths below 4000Å. The spectral half-maxima of the elements at the front end of the aspect telescope are at approximately 4000Å and 4700Å. Additional blocking is provided by the analysis filters.

A.3. *Analysis filters*

The Aspect Telescope package includes two interference filters in the filter wheel near the focal-plane end of the telescope. The "narrowband" filter has a center wavelength at 4310Å, bandpass (FWHM) of 28Å, and maximum transmission of 33%. It was chosen to show the chromospheric network as well as possible. The "broadband" filter is characterized by 4616Å, 184Å, and 2.2%. Both surfaces of each interference filter are anti-reflection coated at their respective center wavelengths. These filters, plus the spectral response of the CCD detector itself, determine the wavelength of observation. Figure 7 of Tsuneta (1991) shows these filter responses.

The in-flight "flat field" calibration of the CCD is done with an opal glass diffuser at one of the positions of the filter wheel. This provides approximately uniform illumination (few percent rms) with sunlight over the CCD area, in the spectral band defined by the pre-filter and lens assemblies. To match signal levels, this opal glass diffuser has an additional attenuator with $\sim$50% transmission.

A.4. *Radiation resistance*

Materials resistant to radiation damage were chosen for all optical components of the SXT aspect telescope where it was practical. The entrance filter used synthetic fused silica, because it has additional resistance to radiation damage from UV, neutrons, protons, electrons, or γ-rays as compared with crushed fused silica or fused quartz. The CM-500 substrate of the bandass filter needed further investigation because radiation damage information was not available before launch. Accordingly Grillot & Rosenberg (1990) conducted successful radiation-damage tests of this material and the Schott equivalent BG-39, with doses as high as 100$\times$the expected three-year dosage for the planned *Yohkoh* orbit. In the design of the SXT aspect telescope, the first element of the system shields the CM-500 element from electrons. The substrates of the analysis filters are cerium-stabilized BK7-G18 material.

A.5. *Control of ghost images*

The white-light attenuator and the bandpass filter elements 0.5-degree tilts in opposite directions to eliminate ghost images over a field of view larger than the Sun. Near the focal plane, however, the problem of suppressing the ghost images is more complex. The uncovered surface of the CCD reflects a portion of the incident light. Anti-reflection

coatings were not possible because of concern about the soft X-ray quantum efficiency. The focal-plane filters are about 20% reflective and 10% absorbing. The reflection will thus be partially reflected back onto the CCD to form a secondary image. Measurements indicated that the CCD was approximately 25% reflective at 4310Å and at 4600Å, which would yield a 5% ghost. This ghost cannot be eliminated from the solar image by tilting the focal-plane filters relative to the CCD because of proximity. However, by incorporating an attenuating glass filter onto CCD-facing side of the focal-plane filters this ghost image intensity was reduced to approximately 1% or less of the primary image intensity. This was accomplished with 2.5 mm thick pieces of Schott UG-5 absorbing glass in each of the two focal-plane filters.

REFERENCES

ANWAR, B., ACTON, L.W., HUDSON, H.S., MAKITA, M., MCCLYMONT, A.N. & TSUNETA, S. 1993 Rapid sunspot motion during a solar flare. *Solar Phys.* **147**, 287–303.

BUFFINGTON, A., HUDSON, H.S. & BOOTH, C.H. 1990 A laboratory measurement of CCD photometric stability and dimensional stability. *Publ. Ast. Soc. Pacific* **102**, 688–697.

CANFIELD, R.C., HUDSON, H.S., LEKA, K.D., ACTON, L.W., STRONG, K.T., KOSUGI, T., SAKAO, T., TSUNETA, S., CULHANE, J.L., PHILLIPS, A. & FLUDRA, A. 1992 The X flare of 1991 November 15: coordinated Mees/*Yohkoh* observations. *Publ. Astr. Soc. Japan* **44**, L111–L115.

DANIELSON, J. 1961 The structure of sunspot penumbras. I. Observations. Ap. J. **134**, 275–288.

FRÖHLICH, C., FOUKAL, P., HICKEY, J., HUDSON, H. & WILLSON, R. C. 1991 Solar irradiance variability from modern measurements. In *The Sun in Time* (ed. C.P. Sonett, M.S. Giampapa & M.S. Mathews). pp. 11–29. Univ. Arizona Press, Tucson, AZ, USA.

GRILLOT, P. & CRUZ, T. 1989 Soft X-ray telescope aspect telescope design note # 31. (unpublished).

GRILLOT, P.N. & ROSENBERG, W.J. 1990 Proton radiation damage in optical filter glass. *Applied Optics* **28**, 4473–4477.

HUDSON, H.S. 1988 Observed variability of the solar luminosity. *Ann. Revs. Astron. Astrophys.* **26**, 473–501.

HUDSON, H.S., ACTON, L.W., HIRAYAMA, T. & UCHIDA, Y. 1992 White-light flares observed by *Yohkoh*. *Publ. Astr. Soc. Japan* **44**, L77–L81.

NEWKIRK, G. 1992 Variation of the solar luminosity. *Ann. Revs. Astron. Astrophys.* **21**, 429–467.

NISHIKAWA, J. 1994 On the cause of total irradiance variability observed by the CCD solar surface photometer., submitted to *Solar Phys.*.

RIBES, E., BEARDSLEY, B., BROWN, T.M., DELACHE, PH., LACLARE, F., KUHN, J.R. & LEISTER, N.V. 1991 The variability of the solar diameter. in *The Sun in Time* (ed. C.P. Sonett, M.S. Giampapa & M.S. Mathews), pp. 59–97. Univ. Arizona Press, Tucson, AZ, USA.

SHIBATA, K. 1994 The variable structure of the X-ray corona as viewed by *Yohkoh*. (ed. J.M. Pap, C. Fröhlich, H.S. Hudson & S.K. Solanki). Cambridge Univ. Press, in press.

TITLE, A., TARBELL, T.D., TOPKA, K.P., FERGUSON, S.H., SHINE, R.A. & THE SOUP TEAM 1989 Statistical properties of solar granulation observed by the SOUP instrument on Spacelab-2. *Ap. J.* **336**, 475–494.

TSUNETA, S., ACTON, L, BRUNER, M., LEMEN, J., BROWN, W., CARAVALHO, R., CATURA, R., FREELAND, S., JURCEVICH, B. MORRISON, M., OGAWARA, Y., HIRAYAMA, T. & OWENS, J. 1991 The soft X-ray telescope for the *Solar-A* mission. *Solar Phys.* **136**, 37.

VAN DRIEL, L. G., HUDSON, H.S., ANWAR, B., HIEI, E. & TSUNETA, S. 1994 A diagnostics of solar atmospheric models: Search for black flares. *Solar. Phys.*, in press.

WILLSON, R.C., GULKIS, S., JANSSEN, M., HUDSON, H.S. & CHAPMAN, G.A. 1981 Observations of solar irradiance variability. *Science* **211**, 700.